Available online at www.derpharmachemica.com

ISSN 0975-413X
CODEN (USA): PCHHAX

Der Pharma Chemica, 2017, 9(20):76-85
(http://www.derpharmachemica.com/archive.html)

Anticarcinogenic Effects and Design of Dinuclear Chelates of New Guanidine Derivatives

Sabreen Mohamed El-Gamasy[1*], Samar Ebrahim Abd-El Razek[2]

[1]Department of Chemistry, Faculty of Science, El-Menoufia University, Shebin El-Kom, Egypt
[2]Department of Clinical Pathology, National Liver Institute, Menoufia University, Shebin El-Kom, Egypt

ABSTRACT

New series of dinuclear transion metal chelates of guanidine ligand have been synthesized and characterized by spectroscopic measurements such as: [1]H-NMR, mass spectra, IR, UV-Visible, ESR, magnetic moments and conductance measurements, as well as elemental and thermal curves (DTA and TGA). The IR data clarify that, the Schiff base is a neutral bidentate or monobasic bidentate ligand attached to the ions of metal through the (N) atom of azomethine and (O) atom of hydroxyl in deprotonated or protonated form adopting tetragonal distorted octahedral geometries. Solutions of molar conductances in DMF clarified that, the chelates are not electrolytes. The ESR spectra of solid Cu(II) chelates (2) and (4) show an axial type. However, Mn(II) complex (8) show isotropic type indicating distorted octahedral geometry. Anticarcinogenic effects of the ligand chelates have been carried out. Chelates show enhanced activity in comparison to the ligand of guanidine and standard drug.

Keywords: Guanidine, Chelates, ESR, Thermal analyses (DTA–TGA), Anticarcinogenic effects

INTRODUCTION

Owing to excellent donor properties of guanidines are capable to stabilize various transition metals in several oxidation states which renders them very valuable for bioinorganic chemistry. Guanidines can be categorized by the number of guanidine units or type of the coordinating atom of the non-guanidine function. In bioinorganic chemistry, the most studies used mono(guanidines), then bis- and tris(guanidines) and mixed of guanidines with other donor atom such as nitrogen and sulfur [1-3]. Characterization of guanidine, basic highly due to the positive charge delocalization of CN_3 group, which resonance-stabilizes the cation. Rapidly, moisture sensitive guanidine reaction in the atmosphere gives rise to its corresponding guanidinium [4-6]. Almost studies had been showed dealing with chemistry of derivatives of guanidinum, which had performed as anticancer [7,8] green corrosion inhibitor for mild acidic solution [9], antiglaucoma and cardio tonic effects and polymer synthesis [10,11]. Guanidinum derivatives show as anion-building fragments in designed super molecular receptors [12,13], improving insulin sensitivity [14] and promotion weight loss of a depose tissue in animal models of non-insulin dependent diabetes mellitus [14]. Also, their effect on function of the mitochondria in the cell [15], their mineralization in soils [16]. In enzymatic transformations, the ion of guanidinium participates in a transition state assembly with the substrates reducing the activation energy or stabilization anionic intermediates, and to orient specific substrates based on their electronic behaviour [17]. Our group focuses on design and spectroscopic characterization of antitumor effect of some transition metal chelates of a wide variety. Herein, we report synthesis and characterization of new chelates of guanidinum ligand. These chelates were characterized by elemental analysis spectral, magnetic and conductivity studies as well as thermal analyses (TGA/DTA). The work was extended to study the anticarcinogenic effects of the ligand as well as some of its metal chelates in related with standard drug (Vinblastine).

MATERIALS AND METHODS

Experimental

The chemicals were used without further purification.

Measurements

At the Analytical Unit of Cairo University, Egypt, C, H, N and Cl analyses were determined. Metal ion was determined by using standard gravimetric method [18]. All metal chelates were dried under vacuum over P_4O_{10}. A Perkin-Elmer 683 spectrophotometer (4000-200 cm^{-1}) used to measure the infra-red spectra. But, the spectra of electrons (qualitatively) were recorded on a Perkin-Elmer 550 spectrophotometer. At 25°C with a Bibby conductimeter type MCl measured the conductance of 10-3 molar solutions of the chelates. Perkin-Elmer R32-90-MHz spectrophotometer using TMS as internal standard measured ^{1}H-NMR spectra (ligand and its Cd(II) chelate). JEULJMS-AX-500 mass

spectrometer recorded spectrum of the mass ligand. From 27 to 800°C at a heating rate of 10°C per min, the thermal analyses (DTA and TGA) were carried out in air on a Shimadzu DT-30 thermal analyzer. The Gouy method using mercuric tetrathiocyanato cobalt(II) measured magnetic susceptibilities at 25°C. Diamagnetic corrections were estimated from Pascal's constant [19]. From this Equation:

$$\mu_{eff} = 2.84\sqrt{\chi_M^{corr}.T}$$

We calculate the magnetic moments. A Varian E-109 spectrophotometer recorded the ESR spectra of solid chelates, but a standard material used DPPH. The purity of all chelates was confirmed using the TLC.

Synthesis of the ligand [H_2L], (1)

[H_2L], (1), for 2 h with stirring, was prepared by refluxing thiourea (25 g, 0.3228 mol) and hydrazine hydrate (16.42 g, 0.3284 mol) in ethanol (100 cm^3). Filter the product to separate the hydrazide after cooling at room temperature. 2-hydroxy-3-methylbenzaldehyde (18.76 g, 0.1378 mol) was reacted with the hydrazide crystals (8 g, 0.0689 mol) and refluxed with stirring for 3 h, ethanol was used to wash the yellow precipitate several times. It was dried in vacuum over P_4O_{10}. Table 1 showed analytical data.

Table 1: Analytical and physical data of the ligand [H_2L] and its metal chelates

S. No.	Ligands/Complexes	Color	FW	M.P (°C)	Yield (%)	Anal./Found (Calc.) (%)					Molar conductance Λm ($\Omega^{-1}cm^{2.}$ mol^{-1})
						C	H	N	M	Cl	
1	[H_2L] $C_{18}H_{20}N_6O_2$	Yellow	352.39	215	78	61.35 (60.98)	5.72 (6.10)	23.85 (23.75)	-	-	-
2	[(L)$Cu_2(OAc)_2(H_2O)_6$] $C_{22}H_{36}Cu_2N_6O_{12}$	Dark green	703.65	>300	85	37.55 (37.85)	5.16 (4.91)	11.94 (12.06)	18.06 (17.96)	-	15
3	[(L)$Cu_2(Cl)_2(H_2O)_6$]. H_2O $C_{18}H_{32}Cl_2Cu_2N_6O_9$	Pale green	674.48	>300	67	32.05 (32.4)	4.78 (4.65)	12.46 (12.51)	18.84 (18.46)	10.51 (10.63)	13
4	[(H_2L)$Cu_2(SO_4)_2(H_2O)_6$].$2H_2O$ $C_{18}H_{36}Cu_2N_6O_{18}S_2$	Dark green	815.73	>300	70	26.50 (25.98)	4.45 (4.34)	10.30 (10.19)	15.58 (15.32)	-	12
5	[(L)$Cu_2(NO_3)_2(H_2O)_6$]. $2H_2O$ $C_{18}H_{34}Cu_2N_8O_{16}$	Pale brown	745.6	>300	75	29.00 (29.17)	4.60 (4.43)	15.03 (15.75)	17.05 (17.02)	-	14
6	[(L)$Ni_2(OAc)_2(H_2O)_6$]. H_2O $C_{22}H_{38}N_6Ni_2O_{13}$	Green	711.96	>300	81	37.11 (37.45)	5.38 (5.26)	11.80 (11.77)	16.49 (16.5)	-	15
7	[(L)$Co_2(OAc)_2(H_2O)_6$] $C_{22}H_{36}Co_2N_6O_{12}$	Brown	694.42	>300	74	38.05 (38.07)	5.23 (5.15)	12.10 (12.22)	16.97 (16.87)	-	11
8	[$(L)_2Mn_2(OAc)_2(H_2O)_6$]. $2H_2O$ $C_{22}H_{40}Mn_2N_6O_{14}$	Dark green	722.46	>300	67	36.57 (36.68)	5.58 (5.39)	11.63 (11.51)	15.21 (15.37)	-	9
9	[(L)$Zn_2(OAc)_2(H_2O)_6$].$2H_2O$ $C_{22}H_{40}N_6O_{14}Zn_2$	Yellow	743.36	>300	74	35.55 (35.51)	5.42 (5.34)	11.31 (11.21)	17.59 (17.87)	-	10
10	[$(L)_2Cd_2(OAc)_2(H_2O)_6$]. $3H_2O$ $C_{22}H_{42}Cd_2N_6O_{15}$	Orange	855.42	>300	68	30.89 (30.77)	4.95 (4.85)	9.82 (9.91)	26.28 (25.97)	-	16
11	[$(L)Hg_2(OAc)_2(H_2O)_6$]. $3H_2O$ $C_{22}H_{42}Hg_2N_6O_{15}$	Dark green	1031.78	>300	64	25.61 (25.57)	4.10 (3.99)	8.15 (8.57)	38.88 (38.58)	-	17
12	[(L)CuZn$(OAc)_2(H_2O)_6$] $C_{22}H_{36}CuN_6O_{12}Zn$	Dark green	705.49	>300	72	37.45 (37.39)	5.14 (4.91)	11.91 (11.98)	Cu=9.01 Zn=9.27	-	20
13	[(L)NiZn$(OAc)_2(H_2O)_6$].$2H_2O$ $C_{22}H_{40}N_6NiO_{14}Zn$	Pale green	736.67	>300	63	35.87 (35.89)	5.47 (5.21)	11.41 (11.58)	Ni=7.97 Zn=8.88	-	19
14	[(L)MnZn$(OAc)_2(H_2O)_6$].H_2O $C_{22}H_{38}MnN_6O_{13}Zn$	Bright brown	714.9	>300	68	36.96 (26.76)	5.36 (5.71)	11.76 (11.81)	Mn=7.68 Zn=9.15	-	21

Metal chelates synthesis (2)-(14)

Solution of ethanol (30 cm^3) of (5.67 g, 0.0284 mol) of $Cu(OAc)_2.H_2O$, (1L:2M), chelate **(**2) was added to the ligand (1) (5.0 g, 0.0171 mol) in ethanol (50 cm^3), (2.81 g, 0.0284 mol) of $CuCl_2.2H_2O$, (1L:2M), chelate (3), (4.53 g, 0.0284 mol) of $CuSO_4.5H_2O$ (1L:2M), chelate (4), (6.86 g, 0.0284 mol) of $Cu(NO_3)_2.3H_2O$, (1L:2 M), chelate (5), (7.06 g, 0.0284 mol) of $Ni(OAc)_2.4H_2O$, (1L:2M), chelate (6), (7.07 g, 0.0284 mol) of $Co(OAc)_2.4H_2O$, (1L:2M), chelate (7), (6.96 g, 0.0284 mol) of $Mn(OAc)_2.4H_2O$, (1L:2M), chelate (8), (6.23 g, 0.0284 mol) of $Zn(OAc)_2.2H_2O$, (1L:2M), chelate (9), (7.56 g, 0.0284 mol) of $Cd(OAc)_2.2H_2O$, (1L:2M), chelate (10), (9.04 g, 0.0284 mol) of $Hg(OAc)_2$, (1L:2M), chelate (11), (2.83 g, 0.01419 mol) of $Cu(OAc)_2.H_2O$ and (3.11 g, 0.01419 mol) of $Zn(OAc)_2.2H_2O$, (1L:1M:1L), chelate (12), (3.53 g, 0.01419 mol) of $Ni(OAc)_2.4H_2O$ and (3.11 g, 0.01419 mol) of $Zn(OAc)_2.2H_2O$, (1L:1M:1L), chelate (13), (3.48 g, 0.01419 mol) of $Mn(OAc)_2.4H_2O$ and (3.11 g, 0.01419 mol) of $Zn(OAc)_2.2H_2O$, (1L:1M:1L), chelate (14). Reflux the mixture with stirring for 2-4 h, depending on the behaviour of the metal ion and the anion. Washing the precipitate with ethanol and dried *in vacuo* over P_4O_{10} after filtration. Analytical data are given in Table 1.

Anticarcinogenic activity

In vitro anticarcinogenic activity of the synthesized chelates using SRB assay as the published method [20]. For 24 h, cells were plated in 96-multiwell plate (10^4 cells/well) before the chelates treatment. Using Dimethyl Sulfoxide (DMSO), the chelates concentrations (0, 1.56, 3.125, 6.5, 12.5 and 25 µg/ml) were added to the cell monolayer triplicate wells were prepared for each individual dose. For 48 h at 37°C under 5% CO_2, monolayer cells were incubated with the chelates. Staining with SRB assay after cell fixing and washing. Acetic acid was used to wash excess stain. An Enzyme-linked Immunosorbent Assay (ELISA) reader was used to measure color intensity. The survival curve of each tumor cell line was given from the relation between surviving fraction and drug chelates concentration.

RESULTS AND DISCUSSION

Tables 1-3 reveal that, the chelates are synthesized in (1L:2M) stoichiometric ratio. All the chelates are stable at room temperature, insoluble in common solvents, *viz*: MeOH, EtOH, $CHCl_3$, CCl_4 and $(CH_3)_2CO$ but soluble in DMSO [18,19]. Condensation of tetraamine hydrazide with p-methyl salicyaldehyde (1:2) molar ratio to synthesize $[H_2L]$, (1) as shown in Figures 1 and 2.

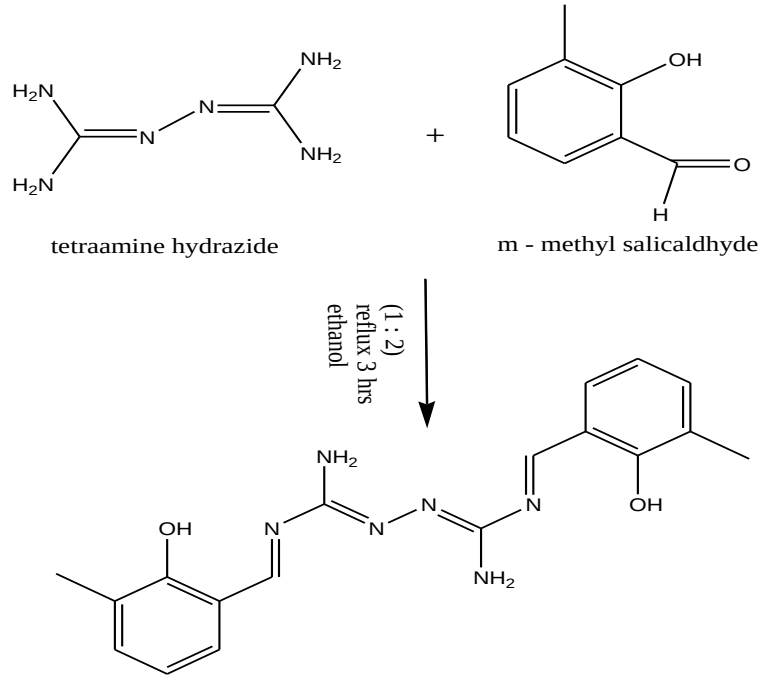

tetraamine hydrazide m - methyl salicaldhyde

ligand (1)

Scheme 1: Ligand synthesis

Scheme 1 formation of strong hydrogen bondings or steric effect of ligand (1) by adding 1:2 molar ratio of tetraamine hydrazide to p-methyl salicyaldehyde (1). Proposed structures of the chelates are shown in Figure 1.

Table 2: Mass spectra of ligand (1) and its Cd(II), chelate (10)

Compound No.	Fragment	m/z	Rel. Int.
(1)	$C_2H_3N_2$	55.03	25
	C_6H_5	77.04	30
	C_7H_7O	107.05	45
	$C_8H_7N_2$	131.06	20
	$C_4H_7N_6$	139.07	35
	$C_{10}H_9N_4$	185.08	40
	$C_{16}H_{13}N_4$	261.11	26
	$C_{18}H_{17}N_4$	289.14	27
	$C_{18}H_{17}N_4O_2$	321.14	18
(10)	$C_2H_3N_2$	55.03	18
	$C_2H_3O_2$	59.02	13
	$C_8H_7N_2$	131.06	17
	C_7H_5NOCd	232.94	22
	$C_4H_7N_6OCd_2$	382.87	26
	$C_{16}H_{13}N_6O_2Cd_2$	548.92	30
	$C_{20}H_{21}N_6O_4Cd_2$	636.97	28

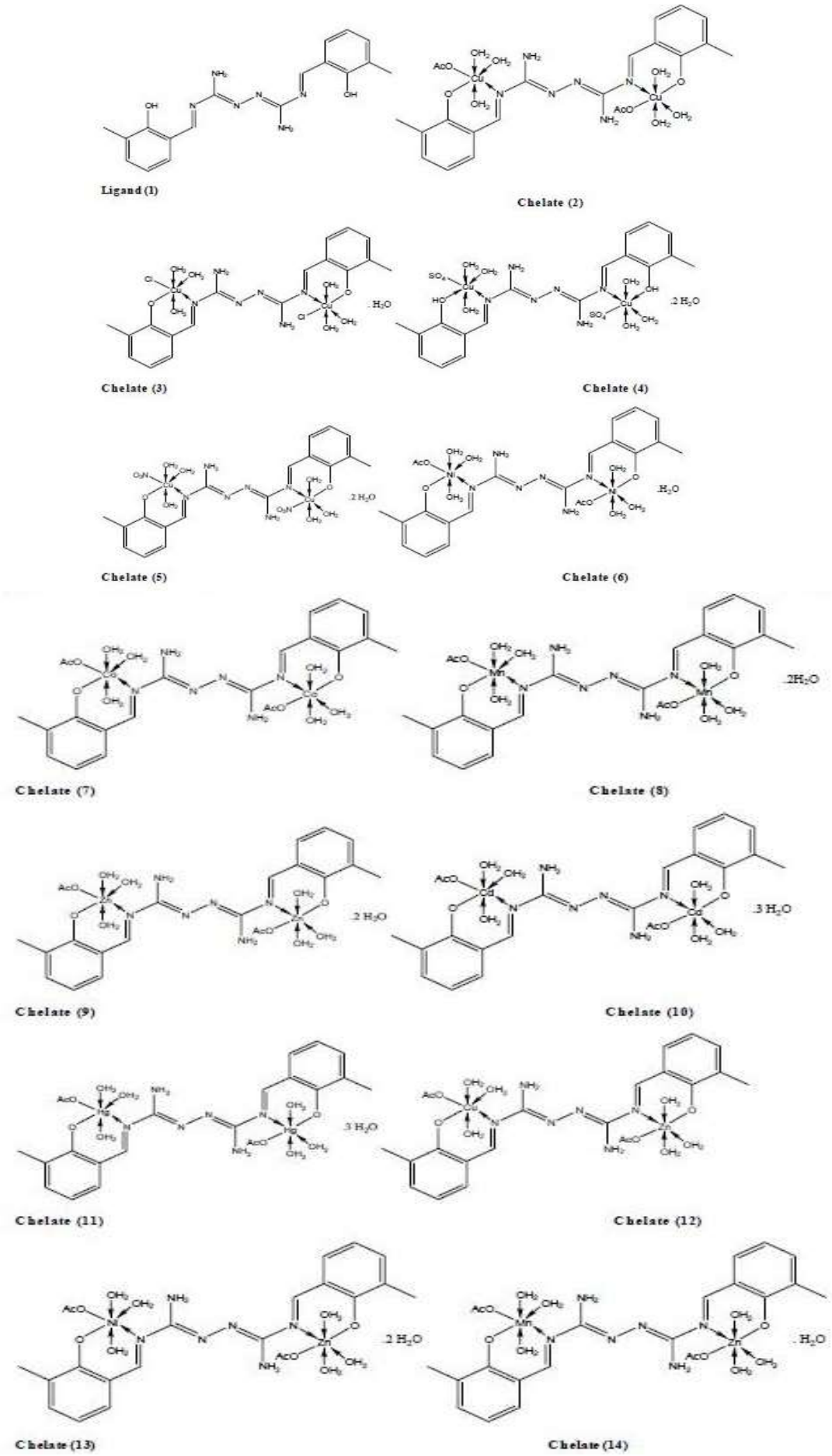

Figure 1: Suggested structures of ligand and its chelates

Table 3: IR frequencies of the bands (cm^{-1}) of ligand [H_2L] and its metal chelates and it`s assignments

S. No.	ν(H_2O/OH)	ν(H-bond.)	N(NH_2)	ν(C=N)	ν(N-N)	ν(Ar)	ν(C-OH)/(C-O)	υ (OAc) /SO_4/ NO_3	υ(M-O)	υ(M-N)	υ(M-Cl)
1	3407, 3380	3610-3205 3190-2850	3316, 3275	1617, 1605	1035	1575, 755 1546, 744	1266, 1225	-	-		-
2	3540-3120	3590-3175 3160-2685	3300, 3255	1603, 1590	1020	1560, 753 1555, 740	1198, 1155	1475, 1320	540	455	-
3	3555-3215 3210-2990	3610-3185 3170-2770	3255, 3235	1614, 1607	1014	1580, 757 1565, 740	1260, 1220	-	582	464	410
4	3390-3375 3560-3200 3180-2840	3588-3150 3120-2657	3374, 3240	1619, 1605	1030	1584, 760 1564, 732	1273, 1245	1125, 1030, 888, 665, 435	560	445	-
5	3644-3260 3240-3080	3592-3175 3165-2875	3345, 3250	1621, 1609	1027	1569, 748 1554, 735	1298, 1236	1377, 1265, 825, 765	570	459	-
6	3630-3214 3200-3050	3585-3170 3160-2690	3275, 3240	1625, 1605	1023	1588, 756 1560, 736	1306, 1265	1480, 1346	515	443	-
7	3610-3250 3235-2980	3575-3164 3150-2650	3335, 3270	1619, 1607	1026	1580, 754 1540, 722	1274, 1235	1465, 1375	563	478	-
8	3620-3260 3250-3005	3590-3120 3100-2805	3357, 3245	1623, 1609	1025	1580, 757 1545, 720	1275, 1236	1443, 1343	554	450	-
9	3650-3322 3300-3105	3560-3300 3100-2755	3355, 3260	1628, 1606	1019	1566, 760 1535, 744	1286, 1237	1450, 1377	525	463	-
10	3600-3225 3200-2980	3610-3125 3100-2857	3320, 3210	1621, 1606	1025	1567, 755 1553, 725	1281, 1199	1442, 1330	509	445	-
11	3587-3155 3120-2857	3610-3165 3150-2710	3330, 3285	1625, 1602	1022	1569, 766 1535, 735	1287, 1235	1430, 1337	584	480	-
12	3600-3260 3250-3050	3580-3150 3130-2655	3370, 3250	1619, 1605	1021	1578, 744 1567, 720	1299, 1222	1480, 1346	565	468	-
13	3617-3160 3130-3008	3580-3200 3180-2750	3406, 3350	1620, 1603	1030	1597, 750 1565, 730	1273, 1189	1430, 1385	558	467	-
14	3605-3250 3235-3100	3600-3150 3120-2805	3350, 3250	1630, 1601	1026	1576, 760 1530, 722	1285, 1199	1465, 1355	580	463	-

Mass spectra

Figure 1 reveals a molecular ion peak (m/z) at 352.39, coincident with the ligand molecular weight. A parent ion peak fragmentations at (m/z)=55.03, 77.04, 107.05, 131.06, 139.07, 185.05, 261.11, 289.14 and 321.14 amu. correspond to $C_2H_3N_2$, C_6H_5, C_7H_7O, $C_8H_7N_2$, $C_4H_7N_6$, $C_{10}H_9N_4$, $C_{16}H_{13}N_4$, $C_{18}H_{17}N_4$ and $C_{18}H_{17}N_4O_2$ moieties, respectively (Table 2). In the chelate **(10),** the mass spectrum suggested its structure, revealed a molecular ion peak (m/z) at 855.42, coincident with the chelate molecular weight. Moreover, the fragmentation pattern splits a parent ion peak at (m/z)=55.03, 59.02, 131.06, 232.94, 382.87, 548.92 and 636.97 amu correspond to $C_2H_3N_2$, $C_2H_3O_2$, $C_8H_7N_2$, C_7H_5NOCd, $C_4H_7N_6OCd_2$, $C_{16}H_{13}N_6O_2Cd_2$, and $C_{20}H_{21}N_6O_4Cd_2$ moieties, respectively (Table 2).

^{1}H-NMR spectra

The ^{1}H-NMR spectra of (1) and its chelate (9) show signals consistent with the suggested structure. The peak of proton of OH group appeared at 11.8 ppm [21,22]. The signals of the protons of CH_3 group observed at 1.31 ppm [21]. The signals of protons of NH_2 group observed at 4.22 and 3.10 ppm [21]. The proton of azomethine group appears at 10.2 ppm [23,24]. The peaks of aromatic protons observed as multiple ones at 6.0-7.9 ppm [23]. The chelate **(9)** spectrum shows, the protons of NH_2 group appeared at 4.11 and 3.09 ppm and the hydroxyl groups (OH) participate in the coordination due to their disappearance in the same position of the ligand [22]. Significant downfield shift appeared at (8.9 ppm) due to complexation of the azomethine proton relative to the free ligand confirms that, the azomethine nitrogen atom coordinates to the metal (N-Zn) [24]. The signals appeared in the 6.1- 8.5 ppm range due to the aromatic protons and new signal was observed at 1.94 ppm due to the protons of the coordinated acetate group [21].

The molar conductivity

Table 1 shows the molar conductance values of the chelates in DMF (10^{-3} M) lie in the 20-9 $\Omega.mol^{-1}.cm^2$ range, observed that, all the chelates are non-electrolytes [21,25]. This indicating that, the coordination between the anion and the metal ion.

Infrared spectra

The bonding modes between (1) and the metal ion can be revealed by comparing the IR spectra of the solid chelates with that of (1). Table 3 shows the infra-red spectral data of the (1) and its metal chelates. In (1), shows broad medium bands in the 3610-3120 and 3190-2650 cm^{-1} ranges, attributed to intra- and intermolecular hydrogen bonds between NH_2 with C=N groups. Thus, the higher frequency band due to a weaker hydrogen bond and the lower frequency band due to a stronger hydrogen bond. The stretching vibrations of the amino $\nu(NH_2)$ associated through intermolecular and intramolecular bondings show bands in the 3406-3210 cm^{-1} range [26,27]. Strong bands of the ν(C=N) imine and $\nu(C=C)_{Ar}$ are located at 1617, 1605 and 1575, 755 and 1546, 744 cm^{-1} [28]. The decreasing intensity shifted the band due to azomethine ν(C=N) imine, indicating its coordination to the central metal ion in all chelates [29,30]. The bands appeared in the 3406-3210 and 1597-1530 and 766-720 cm^{-1} ranges due to $\nu(NH_2)$ and $\nu(C=C)_{Ar}$ groups, respectively [31,32]. The bands of the hydrated or coordinated water molecules appeared at 3644-3120 and 3300 - 2840 cm^{-1} ranges [33]. However, the bands of intra- and intermolecular hydrogen bondings appeared at 3610-3120 and 3190-2650 cm^{-1} ranges [28,29,32]. New bands observed in the 582-509 and 480-443 cm^{-1} ranges indicated to the coordination between the metal ions with O and N atoms, respectively [30,31]. Complex (3) shows band at 410 cm^{-1} is due to the monodentate chloride anion ν(M-Cl) [33,34]. The data of IR spectra showed on metal acetate chelates [30] indicating, the coordination of acetate ligand [30] in either a monodentate, bidentate or bridging manner, the νa(COO) and νs(COO) of the free acetate are at 1565 and 1424 cm^{-1}, respectively. In monodentate, coordination ν(C=O) is at higher energy than νa (COO) and ν(C-O) is lower than νs(COO). As a result, the separation between ν(CO) bands is much larger in monodentate complexes. In chelates (2) and (6-14) the bands is due to νa(COO) appeared in the 1480-1430 cm^{-1} and the νs(COO) appeared in the 1385-1320 cm^{-1} ranges. The acetate group coordinates in unidentate manner with the metal ions due to the difference between these two bands is in the 50-65 cm^{-1} range [28]. Chelate (5) shows bands at (1377, 1265, 825, 765) cm^{-1} assigned to coordinated nitrate group [29,30]. Chelate (4), bands values at (1125, 1030, 888, 665, 435) cm^{-1} indicate that the sulphate ion is coordinated to the metal ion in a unidentate chelating fashion [33,35]. The $\nu(NH_2)$ group appeared at higher wave number comparing to the ligand indicating that it is not coordinate the metal ion.

Transitions of electrons

At room temperature, DMF electronic spectral bands and effective magnetic moment values of (1-14) are shown in Table 4. (H_2L) (1) Showed three transition bands in the high energy region. The aromatic rings band appeared at 265 nm, due to unchanged upon complexation. The other bands appearing at 320 and 385 nm may be assigned to $n \rightarrow \pi^*$ of the azomethine groups and CT transitions [36-39]. The bands were found to be shifted upon complexation indicate to involve of theses transition in the coordination with the metal ions. The spectra of the electrons of chelates (2-5) exhibited bands in the 645-660, 575-585 and 420-445 nm ranges which are due to $^2B_1g \rightarrow {}^2A_1g$ ($d_{(x2-y2)} \rightarrow d_{z2}$), and $^2B_1g \rightarrow {}^2Eg$ ($d_{(x2-y2)} \rightarrow d_{xy}$, d_{yz}) transitions, respectively. These transitions indicating the Cu(II) ion has a tetragonal distorted octahedral geometry because of the operation on the d^9 electronic ground state of six coordinate system to elongate one trans pair of coordinate bonds and shortening the remaining four ones [35,37]. The magnetic moments for all chelates (2-5) are in the 1.69-1.75 B.M. range, indicating that, the complexes have square planar and octahedral geometry [40]. The electronic absorption spectra of chelate (6) appeared three bands at 498, 625, 755 nm, these bands are corresponding to ^3A_2g (F) $\rightarrow {}^3T_2g$ (F)(1), ^3A_2g (F) $\rightarrow {}^3T_1g$(F)(2) and ^3A_2g (F) $\rightarrow {}^3T_1g$(P)(3) transitions, respectively, indicating octahedral of these chelates [37,39]. The lower value of 2/1 ratio for the chelates (1.27-1.34) range which are less than the usual range of 1.5-1.75, indicating distorted octahedral Ni(II) chelate. The magnetic moment values of chelate (6) is 2.86 BM, respectively, which are consistent with two unpaired electrons state and confirming octahedral geometry for around the Ni(II) ion [38]. The spectra of the electrons of the chelate (7) show three d–d transition bands at 550, 617, 730 nm. These bands are assigned to $^4T_1g(F) \rightarrow {}^4T_2g(F)(1)$, $^4T_1g(F) \rightarrow {}^4T_1g(p)(2)$, $^4T_1g(F) \rightarrow {}^4A_1(F)$ (3) transitions, respectively, corresponding to high spin Co(II) octahedral chelates [38,39]. The magnetic moment of chelate (7) is 3.45 B.M., which is well within the reported range of high spin octahedral Co(II) chelates. The spectrum of absorption of chelate (8) showed bands at 455, 515, 615 nm. The last two bands can be assigned to $^5B_1g \rightarrow {}^5Eg$ and $^6B_1g \rightarrow {}^6A_2g$ transitions, respectively, suggesting an distorted octahedral arrangement around the manganese(II) ion [41,42]. The magnetic moment values for the chelate (8) are 4.95 B.M., which is consistent with a high spin octahedral geometry around the Mn(II) ion [41,42]. The mixed chelates (12-14) give bands indicating octahedral structures and diamagnetic Zn(II), Cd(II) and Hg(II) chelates which give only intraligand transitions are reported in Table 4.

Table 4: The electronic absorption spectral bands (nm) and magnetic moment (B.M) for the ligand [H_2L] and its chelates

S. No.	λ_{max} (ε)	μ_{eff} in BM
1	265 (ε=6.15 × 10^{-3} $mol^{-1}.cm^{-1}$) 320 (ε=7.69 × 10^{-3} $mol^{-1}.cm^{-1}$) 385 (ε=9.36 × 10^{-3} $mol^{-1}.cm^{-1}$)	-
2	255, 323, 389, 420, 581, 660	1.72
3	260, 320, 385, 428, 585, 645	1.74
4	255, 324, 390, 424, 582, 649	1.75
5	260, 318, 387, 445, 575, 645	1.69
6	260, 315, 385, 498, 625, 755	2.86
7	250, 325, 390, 550, 617, 730	3.45
8	265, 315, 370, 455, 515, 615	4.95
9	260, 320, 370	Dia
10	265, 315, 380	Dia
11	265, 325, 387	Dia
12	265, 315, 390, 450, 540, 630	1.96
13	270, 325, 383, 448, 535, 635	3.77
14	270, 318, 385, 455, 540, 620	5.11

*in nm

Thermal analyses (DTA and TGA)

The thermal analyses (DTA and TGA) were listed in Table 5. In the temperature 27-800°C range, the thermal curves of chelates (2), (4), (8) and (10) are stable up to 35°C. The endothermic peaks of dehydration characterized by within the temperature 70-90°C range due to the loss of hydrated water molecules [43,44]. Chelate (2), the decomposition step started with the breaking of H-bonding accompanied with endothermic peak at 43°C, followed by the elimination six coordinated water molecules through endothermic peak at 135°C, with 15.26% weight loss (Calc. 15.35%). However, the peak observed at 185°C with 19.55% weight loss (Calc. 18.81%), assigned to two acetate groups. The endothermic peak

observed at 315°C may be assigned to the melting point. The decomposition of the oxides occurs in the 430-660°C range with exothermic peaks, leaving CuO 32.98% weight loss (Calc. 33.28%) [43,44]. The decomposition step for chelate (4) starting with the breaking of H-bonding accompanied with endothermic peak at 45°C, followed by the elimination of two hydrated water molecules ($2H_2O$) at 80°C with 4.33% weight loss (Calc. 4.41%), followed by the elimination six coordinated water molecules through endothermic peak at 140°C, with 13.76% weight loss (Calc. 13.89%). Another thermal decomposition peaks at 210°C with 28.48% weight loss (Calc. 28.58%), which could be due to the loss of two coordinated sulphate groups. Also, Endothermic peak observed at 330°C with no weight loss may be due to melting point. Also, the chelate shows exothermic peaks in the 430-610°C range, due to oxidative decomposition gives final residue at 610°C, assigned to CuO [44,45].

The decomposition step for chelate (8) starting with the breaking of H-bonding accompanied with endothermic peak at 46°C, followed by the elimination of two hydrated water molecules ($2H_2O$) at 85°C with 4.67% weight loss (Calc. 4.98%) and then the elimination six coordinated water molecules through endothermic peak at 130°C, with 15.62% weight loss (Calc. 15.73%). However, the peak observed at 175°C with 20.23% weight loss (Calc. 20.39%), assigned to two acetate groups. The endothermic peak observed at 340°C may be assigned to the melting point. The decomposition of oxides appears at the 450-660°C range with exothermic peaks, leaving MnO 30.79% weight loss (Calc. 30.81%) [43,44]. The decomposition step for chelate (10) starting with the breaking of H-bonding accompanied with endothermic peak at 44°C, followed by the elimination of three hydrated water molecules ($3H_2O$) at 90°C with 6.11% weight loss (Calc. 6.31%) and then the elimination six coordinated water molecules through endothermic peak at 145°C, with 13.25% weight loss (Calc. 13.48%). However, the peak observed at 180°C with 16.89% weight loss (Calc. 17.02%), assigned to two acetate groups. The endothermic peak observed at 310°C may be assigned to the melting point. The decomposition of oxides occurs in the 455-670°C range with exothermic peaks, leaving CdO 44.54% weight loss (Calc. 44.22%) [44,45].

Table 5: Thermal data for some of metal chelates

Compound	Temperature (°C)	DTA (peak)		TGA (Weight loss)		Assignments
		Endo and Exo calculation found				
Chelate (2)	43	Endo	-	-	-	Broken of H-bondings
	135	Endo	-	15.35	15.26	Loss of ($6H_2O$) coordinated water molecules
	185	Endo	-	19.81	19.55	Loss of coordinated two (OAc) groups
	315	-	Exo	-	-	Melting point
	430-660	-	Exo	33.28	32.98	Decomposition process with formation of CuO
Chelate (4)	45	Endo	-	-	-	Broken of H-bondings
	85	Endo	-	4.41	4.33	Loss of ($2H_2O$) hydrated water molecules
	140	Endo	-	13.89	13.76	Loss of ($6H_2O$) coordinated water molecules
	210	Endo	-	28.58	28.48	Loss of coordinated two (SO_4) groups
	330	Exo	-	-	-	Melting point
	430-610	-	Exo	33.14	32.82	Decomposition process with the formation of CuO
Chelate (8)	46	Endo	-	-	-	Broken of H-bondings
	85	Endo	-	4.98	4.67	Loss of ($2H_2O$) hydrated water molecules
	130	Endo	-	15.73	15.62	Loss of ($6H_2O$) coordinated water molecules
	175	Endo	-	20.39	20.23	Loss of coordinated two (OAc) groups
	340	Endo	-	-	-	Melting point
	450-660	-	Exo	30.81	30.79	Decomposition process with the formation of MnO
Chelate (10)	44	Endo	-	-	-	Broken of H-bondings
	90	Endo	-	6.31	6.11	Loss of($3H_2O$) hydrated water molecules
	145	Endo		13.48	13.25	Loss of coordinated two (OAc) groups
	180	Endo	-	17.02	16.89	Loss of two (OAc) groups
	310	Exo	-	-	-	Melting Point
	455-670	-	Exo	44.63	44.22	Decomposition process with the formation of CdO

Electron spin resonance analyses

In Table 6 presented the ESR data of chelates (2), (4), (6), (8), (12) and (14). The spectra of chelates (2) and (4) are characteristic of species, d9 configuration and having axial type of a d(x2-y2) ground state which is the most common for Cu(II) chelates [46,47]. The chelates showed $g_{\|}>g_{\perp}>2.0023$, indicate to octahedral geometry around the Cu(II) ion [48]. The expression G is related to g-values, $G=(g_{\|}-2)/(g_{\perp}-2)$. If G>4.0, then local tetrahedral axes are misaligned parallel or only slightly misaligned and if G<4.0, significant exchange coupling is present [49]. The $g_{\|}/A_{\|}$ values lie just within the range expected for the square planar or octahedral chelates [50]. The orbital reduction factors ($K_{\|}$, $K_{\perp}$, K), which are a measure of covalence were also calculated [51]. K values, for the chelates (2) and (4), indicate to covalent bond character [51]. Also, the g-values show considerable a covalent bond character. The in-plane σ-covalence parameter, α2 (Cu) suggests a covalent bonding. The chelates (2) and (4) show^2 β_1 values indicating a covalence character in the in-plane π-bonding. While β^2 for the chelates indicating an ionic bonding character in the out of plane π-bonding, however chelate (4) shows ionic bond character out of plane bonding [49,51]. The calculated orbital populations (a^2d) for the Cu(II) chelate indicate a d(x2-y2) ground state [51]. Mn(II) chelate (8) and mixed metal chelates (12) and (14) show isotropic spectra with 2.15, 2.08 and 2.007 values, respectively.

Table 6: ESR data for the metal (II/III) chelates

S. No.	$g_{\|}$	$g_{\perp}$	g_{iso}[a]	$A_{\|}$ (G)	$A_{\perp}$ (G)	A_{iso}[b] (G)	G[c]	ΔE_{xy}	ΔE_{xz}	$K_{\perp}^2$	$K_{\|}^2$	K	$g_{\|}/A_{\|}$	α^2	$ß^2$	$ß_1^2$	-2 ß	a_d^2 (%)
(2)	2.14	2.06	2.08	160	10	16	2.17	19606	23809	0.83	o.38	o.68	0.82	134	0.62	1.32	180	75
(4)	2.20	2.05	2.10	140	20	60	4.0	15456	19268	0.56	0.46	0.73	157.1	0.64	0.87	0.72	303	90
(6)	2.27	2.07	2.14	150	15	65	3.86	15625	19802	0.64	0.8	0.83	142.7	0.78	0.82	1.02	244.3	72.8
(8)	-	-	2.15	-	-	-	-	-	-	-	-	-	-	-	-	-	-	-

(12)	-	-	2.08	-	-	-	-	-	-	-	-	-	-	-	-	-	-	-
(14)	-	-	2.007	-	-	-	-	-	-	-	-	-	-	-	-	-	-	-

(a) $g_{iso}=(2g_{\perp}+g_{\parallel})/3$, (b) $Aiso=(2A_{\perp}+A_{\parallel})/3$, c) $G=(g_{\parallel}-2)/(g_{\perp}-2)$

Anticarcinogenic effects

The anticarcinogenic effects of the [H_2L], (1) and its chelates against HepG-2 cell lines of **(**hepatic cellular carcinoma) was evaluated by using the (SRB) assay method under concentrations ranged from 0.1-100 µg/ml. The IC_{50} values obtained of ligand and its complexes are depicted in Figure 2 and listed in Table 7. After the incubation of tumor cells, in the presence of the tested chelates for 48 h, the IC_{50} values for all of ligands and chelates ranged from 4.82-50 µg/ml against HepG-2, indicating varying degree of antitumor activity of the ligand and its chelates. It was reported that comps exhibiting IC_{50} values more than 10-25 µg/ml indicate weak cytotoxic activities while chelates with IC_{50} values less than 5 µg/ml are considered to be very active. Those having intermediate values ranging from 5-10 µg/ml are classified as moderately active [52,53]. Accordingly, the IC_{50} values refer to a strong cytotoxic activity of the ligand against HepG-2 with IC_{50} (30.6 and 16 µg/ml)**.** It is worth noting, the cytotoxic activity was enhanced upon complexation of the ligand to the metal ions. It was interestingly found that the Cu(II) chelates (2), (4) and (5), Co(II) chelate (7), Zn(II) chelate (9) and mixed chelates (12), (13) and (14) formed in (1L:2M) ratios, recorded the highest cytotoxicity against HepG-2 with IC_{50} 11.02, 8.05, 13.4, 10.05, 14.33, 12.33 17.8 and 9.24, respectively which are presented in Table 8 and Figure 3. The cytotoxicity of the ligand and its metal complexes of both was found to be concentration dependent, the cell viability decreased with increasing the concentration of the chelates [44-54]. The resulting concentration–effect obtained with continuous exposure for 48 h are depicted in Figure 2.

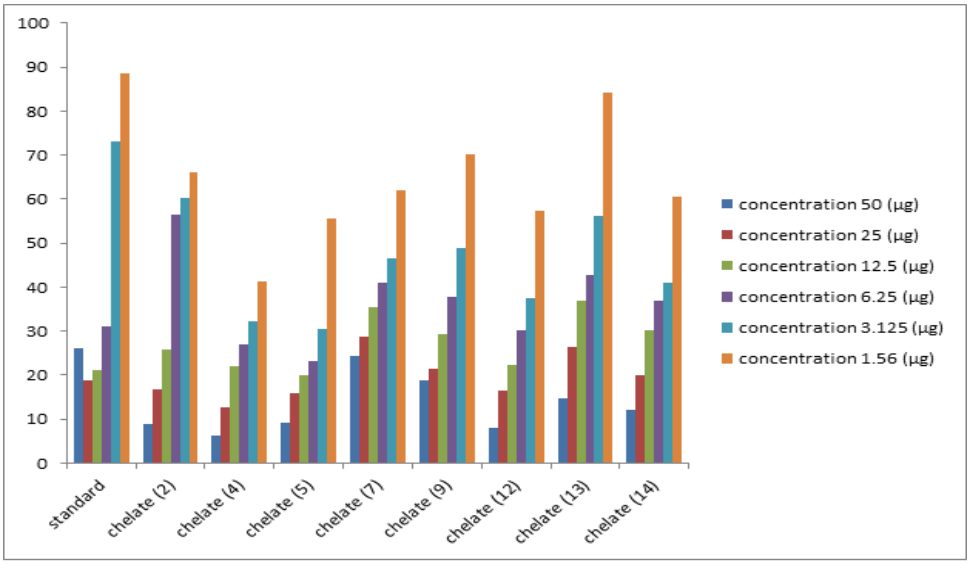

Figure 2: The anticarcinogenic effects of chelates (2), (4), (5), (7), (9), (12), (13) and (14) against HEPG-2 cell line

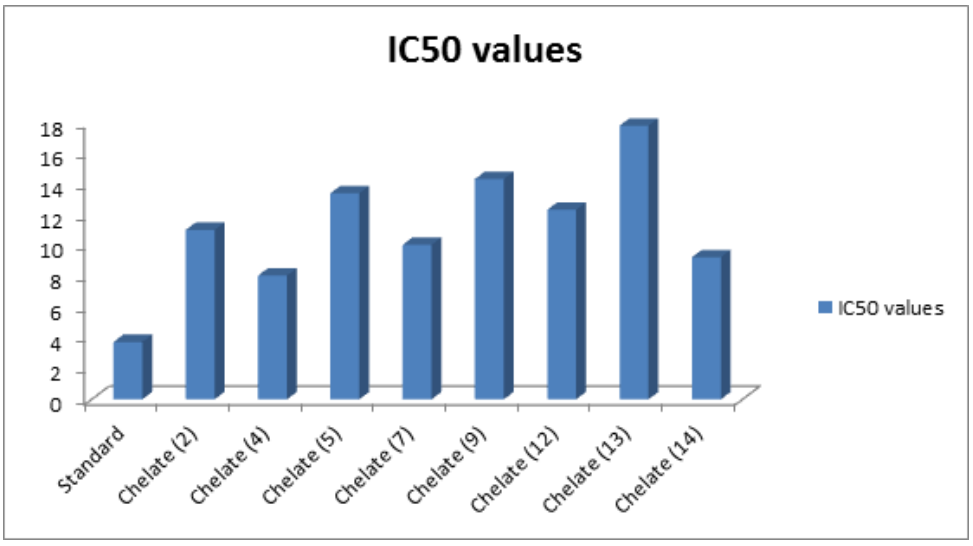

Figure 3: IC_{50} values of some chelates (2), (4), (5), (7), (9), (12), (13) and (14) against human hepatocellular carcinoma cells (HepG-2)

Table 7: The Antiproliferative activity of chelates (2), (4), (5), (7), (9), (12), (13) and (14) against HEPG-2 cell line

Chelates	standard	chelate (2)	chelate (4)	chelate (5)	chelate (7)	chelate (9)	chelate (12)	chelate (13)	chelate (14)
concentration 50 (µg)	26.21	8.88	6.36	9.12	24.25	18.74	8.14	14.68	12.02

concentration 25 (µg)	18.89	16.82	12.65	15.88	28.87	21.33	16.59	26.41	19.87
concentration 12.5 (µg)	21.19	25.89	22.03	19.89	35.46	29.26	22.23	37.05	30.16
concentration 6.25 (µg)	31.18	56.42	27.06	23.22	40.99	37.74	30.28	42.63	36.78
concentration 3.125 (µg)	73.12	60.15	32.13	30.45	46.56	48.85	37.55	56.24	40.99
concentration 1.56 (µg)	88.5	66.18	41.21	55.47	62.05	70.09	57.41	84.11	60.45

Table 8: IC_{50} values of some metal chelates (2), (4), (5), (7), (9), (12), (13) and (14) against human hepatocellular carcinoma cells (HepG-2)

Chelates No.	IC_{50} values
Standard	3.73
Chelate (2)	11.02
Chelate (4)	8.05
Chelate (5)	13.4
Chelate (7)	10.05
Chelate (9)	14.33
Chelate (12)	12.33
Chelate (13)	17.8
Chelate (14)	9.24

CONCLUSION

Novel metal complexes derived from new ligand have been successfully prepared and spectrally characterized. Based on spectroscopic methods as well as magnetic moment measurements, the proposed geometries of the complexes are distorted octahedral around metal ions in nature. The antitumor activity results revealed that the ligand showed a weak inhibition effect against hepatocellular carcinoma cell lines (HEPG-2), on the other hand, the metal complexes showed outstanding high activities against (HEPG-2) cell line.

ACKNOWLEDGEMENT

First of all I should express my deep thanks to ALLAH, without great blessing I should have never accomplished this wok. I would like to express my deep thanks to our Professors of Inorganic Chemistry, Faculty of Science, Menoufia University for the continuous help, guidance, support and encouragement.

REFERENCES

[1] P.J. Bailey, S. Pace, *Coord. Chem. Rev*., **2001**, 214, 91-141.
[2] F.T. Edelmann, *Org. Chem*., **2008**, 57, 183-352.
[3] F.T. Edelmann, *Org. Chem.*, **2013**, 61, 55-374.
[4] W.X. Zhang, L. Xua, Z. Xi, *Chem. Commun.*, **2015**, 51, 254-265.
[5] D. Elorriaga, F.C. Hermosilla, A. Antinolo, F.J. Suarez, I.L. Solera, R. Fernandez-Galan, E. Villaseno, *Dalton. Trans.*, **2013**, 42, 8223-8230.
[6] A. Gobbi, G. Frenking, *J. Am. Chem. Soc*., **1993**, 115, 2362-2372.
[7] L. Meurling, M. Marquez, S. Nilson, A.R. Holmberg, *Int. J. Oncol*., **2009**, 35, 281.
[8] Z. Brozozowski, F. Saczewski, J. Slawinski, *Eur. J. Med. Chem*., **2007**, 42, 1218.
[9] K.F. Khaled, *Int. J. Electrochem. Sci*., **2008**, 3, 462.
[10] O. Benemann, R. Haase, A. Jesser, T. Beschitt, A. Doring, D. Kuckling, I. Vieira, U. Florke, S.H. Pawlis, *Eur. J. Inorg. Chem*., **2011**, 2367.
[11] A. Zhakouskaya, H. Gorls, G. Vaughan, W. Plass, *Inorg. Chem. Comm*., **2005**, 8, 1145.
[12] K.A. Schug, W. Linder, *Chem. Rev*., **2005**, 105, 67.
[13] M.D. Best, S.L. Tobey, E.V. Anshyn, *Coord. Chem. Rev*., **2003**, 240, 3.
[14] M.D. Wilson, J.M. Yau, J.H. Robinson, D.D. Wyse, B.M. Desouza, *J. Pharm. Macol. Exp. Ther*., **1933**, 266, 1454.
[15] F. Davidoff, *J. Biolog. Chem*., **1971**, 246, 4017.
[16] P. Kumar, R. Brumme, *Nut. Cyc. Agroco*., **1999**, 53, 133.
[17] H. Ube, D. Uraguchi, M. Terada, *J. Organomet. Chem*., **2007**, 692, 545.
[18] A.I. Vogel, Longman Suffolk, **1961**.
[19] J. Lewis, R.G. Wilkins, Interscience, New York, **1960**, 403.
[20] P. Skehan, R. Storeng, *J. Natl. Cancer Inst*., **1990**, 82, 1107.
[21] M. Balci, Amsterdam., **2005**, 25-85.
[22] F. El-Mariah, *J. Chem. Res*., **2009**, 588.
[23] S. Mayadevi, P.G. Prasad, K.K.M. Yusuff, *Synth. Rea. Inorg. Met. Org. Chem*., **2003**, 33, 481.
[24] A.S. El-Tabl, R.M. El-Bahnasawy, M.M.E. Shakdofa, A. El-Deen Abdalah, *J. Chem. Res*., **2010**, 88.
[25] W.J. Geary, *Coord. Chem. Rev*., **1971**, 7, 81.
[26] S. Naskar, *Inorg. Chem. Acta.*, **2011**, 371(1), 100-106.
[27] M. Bakheit, S. Satyanarayana, *J. Korean. Chem. Soc*., **2010**, 6(54), 687.
[28] M.F.R. Fouda, A.B.D. El-Zaher, M.M. Shakdofa, F.A. El-Sayed, M.I. Ayad, A.S. El-Tabl, *J. Coord. Chem*., **2008**, 61, 1983.
[29] S.K, Nakamoto, 3rd Ed., John Wiley & Sons, New York, **1977**, 244-247.
[30] N.S, Youssef, E. El-Zahery, A.M.E. El-Seidy, *Phosphorous. Sulfur. Silicon.*, **2010**, 185, 785.
[31] A.S, El-Tabl, F.A. El-Saied, A.N. Al-Hakimi, W. Plass, *Spectro. Chem. Acta.*, **2008**, 67, 265.

[32] A.S. El-Tabl, K. El-Baradie, R.M. Issa, *J. Coord. Chem*., **2003**, 56, 1113.
[33] A.S. El-Tabl, F.A. El-Saied, A.N. Al-Hakimi, *J. Coord. Chem*., **2008**, 61, 2380.
[34] H.A. Kuska, M.T. Rogers, A.E. Martell, *J. Coord. Chem*., **1971**.
[35] A.S. El-Tabl, J.J. Stephanos, M.M. Abd-Elwahed and S.M. El-Gamasy, *Int. J. ChemTech. Res*., **2015**, 5(4), 3875-3908.
[36] H.G. Aslan, S. Özcan, N. Karacan, *Inorg. Chem. Comm*., **2011**, 14(9), 1550-1553.
[37] G.G. Mohamed, M. Omar, A.M. Hindy, *Spectrochim. Acta. Mol. Biomol. Spectrosc*., **2005**, 62(4), 1140-1150.
[38] K.D. Karlin, J. Zubieta, Adenine press, **1983**, 498.
[39] M.A. Akbar, A.H. Mirza, C.Y. Yee, H. Rahgeni, P.V. Bernhardt, *Polyhedron*., **2011**, 30(3), 542-548.
[40] K.R. Surati, *Spectrochim. Acta. Mol. Biomol. Spectrosc*., **2011**, 79(1), 272-277.
[41] B.J. Kennedy, K.S. Murray, *J. Inorg. Chem*., **1985**, 24(10), 1552-1557.
[42] J.A. Bertrand, T.D. Black, P.G. Eller, F.T. Helm, R. Mahmood, *Inorg. Chem*., **1976**, 15, 2965.
[43] A.S. El-Tabl, J.J. Stephanos, M. M.Abd-Elwahed, E. El-Deen Metwally, S.M. El-Gamasy, *J. Chem. Biol. Phys. Sci.*, **2015**, 5(4), 3875-3908.
[44] J.C. Eisenstein, *J. Chem. Phys*., **1958**, 28(2), 323-329.
[45] B.J. Hathaway, D.E. Billing, *Coord. Chem. Rev*., **1970**, 5(2), 143-207.
[46] A.A.G. Tomlinson, B.J. Hathaway, *J. Chem. Soc. A*., **1968**, 1685-1688.
[47] A.S. El-Tabl, F.A. Aly, M.M.E. Shakdofa, A.M.E. Shakdofa, *J. Coord. Chem*., **2010**, 63(4), 700-712.
[48] A.N. Al-Hakimi, A.S. El-Tabl, M.M. Shakdofa, *J. Chem. Res*., **2009**, (12).
[49] N.M., Shauib, A.Z.A. Elassar, A. El-Dissouky, *Spectrochim. Acta. Mol. Biomol. Spectrosc*., **2006**, 63(3), 714-722.
[50] N.N. Greenwood, B.P. Straughan, A.E. Wilson, *J. Chem. Soc. A*., **1968**, (0) 2209-2212.
[51] M.C. Symons, P.M. Trousson, *Radiat. Phys. Chem.*, **1977**, 23(1), 127-135.
[52] E. Ispir, S. Toroglu, A. Kayraldiz, *Trans. Met. Chem*., **2008**, 33, 953.
[53] M. Akbar, A.H. Mirza, C.Y. Yee, H. Rahgeni, P.V. Bernhardt, *Polyhedron.*, **2011**, 30(3), 542-548.
[54] G.M.A. El-Reash, K.M. Ibrahim, M.M. Bekheit, *J. Trans. Met. Chem*., **1990**, 15(2), 148-151.